



ELSEVIER

Journal of Physics and Chemistry of Solids 61 (2000) 461–465

JOURNAL OF  
PHYSICS AND CHEMISTRY  
OF SOLIDS

www.elsevier.nl/locate/jpcs

# An X-ray scattering beamline for studying dynamics

A.Q.R. Baron<sup>\*</sup>, Y. Tanaka, S. Goto, K. Takeshita, T. Matsushita, T. Ishikawa

*SPring-8, 323-3 Mihara, Mikazuki-cho, Sayo-gun, 679-5198, Japan*

## Abstract

We describe the design of an instrument for the investigation of sample dynamics: the SPring-8 High Resolution Beamline (BL35XU). The primary purpose of the beamline is high resolution ( $\sim$ meV) inelastic X-ray scattering measurements. The secondary purpose is nuclear resonant scattering measurements. Construction of the beamline will begin in the summer of 1999 and commissioning will start in the spring of 2000. © 2000 Elsevier Science Ltd. All rights reserved.

*Keywords:* D. Phonons; Synchrotron radiation

## 1. Introduction

The construction of high brilliance, third generation, hard-X-ray synchrotron radiation facilities has made possible the development and advancement of many areas of X-ray scattering. Of these facilities, the European Synchrotron Radiation Facility (ESRF) [1] in Grenoble, France was the first operational one (providing user beam in the fall of 1994) while the Advance Photon Source (APS) [2] near Chicago, IL, began providing X-rays in 1996. Most recently, the Super Photon Ring (SPring-8) [3], in the Kansai region of Japan, began user operation in the Fall of 1997. SPring-8 presently has 16 operating beamlines, of which the majority are public beamlines [4], open for user proposals originating both inside and outside of Japan.

Two of the fields that have benefited greatly from the development of third generation facilities are high resolution inelastic X-ray scattering (IXS) [5] and nuclear resonant scattering (NRS) of synchrotron radiation [6]. Pioneering work in IXS was done at HASYLAB in Hamburg, Germany [7] while the utility of the technique as a probe of condensed matter physics was demonstrated at ESRF [8]. More recently an IXS instrument at APS has begun to provide results [9,10], and a second beamline for these measurements has been built at ESRF [11]. In the field of nuclear resonant scattering of synchrotron radiation, first work was also done at HASYLAB [12]. However, during the period

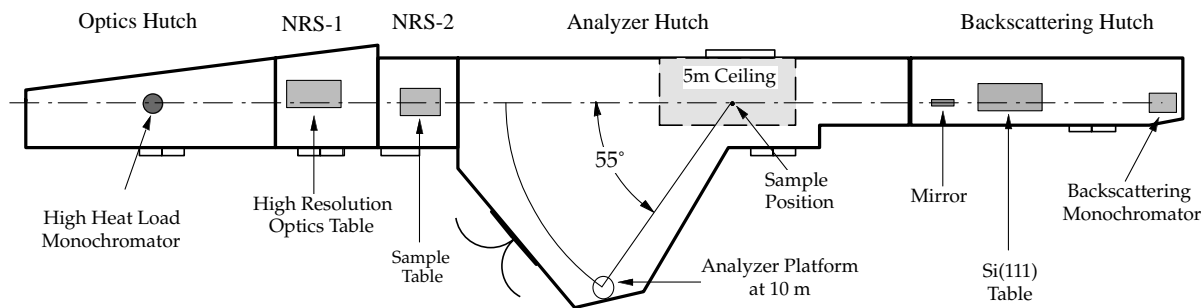
between this first work and the operation of the NRS beamline at ESRF, pioneering experiments were carried out by many groups working in facilities in Europe, the US and Japan [13]. However, construction of beamlines at ESRF [14] and APS [15] have been crucial in expanding the field, with the very recently commissioned beamline 9 at SPring-8 [16] providing the potential to do even more demanding experiments.

The SPring-8 high resolution beamline (BL35XU) will combine IXS and NRS experiments, with an emphasis on measurement of sample dynamics. IXS, being essentially a type of three-axis spectrometry, measures  $S(\mathbf{q}, \omega)$ . Nuclear resonant techniques provide several alternative methods of investigating sample dynamics, the most robust of these being measurement of the phonon density of states [17,18]. The two fields complement each other, allowing slightly different information to be obtained about similar physical properties. They also have strengths for different types of samples.

In this paper we describe the design of BL35XU, a public beamline administered by the Japan Synchrotron Radiation Research Institute (JASRI) and funded through the Japan Atomic Energy Research Institute (JAERI). We provide an introduction to its capabilities and some discussion of the design considerations. At present, the specifications for most of the major components have been finalized, including the insertion device, the hutches, the transport channel, the safety interlock system, the IXS spectrometer, and the NRS optics table. A schematic of the beamline is shown in Fig. 1. Construction of the beamline will begin in the summer of 1999 with commissioning to start in the Spring of 2000.

<sup>\*</sup>Corresponding author. Tel.: +81-7915-8-0802 (ext. 3883); fax: +81-7915-8-2807.

*E-mail address:* baron@spring8.or.jp (A.Q.R. Baron).

**(a) Hutch Layout for BL35XU****(b) Beam Path for IXS**

(Vertical Scattering Plane)

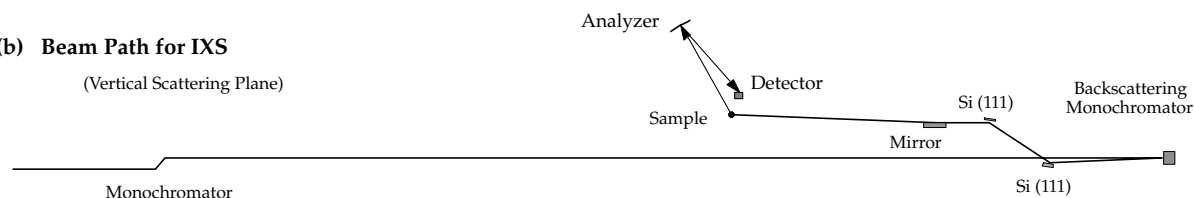


Fig. 1. (a) Hutch layout for BL35XU; and (b) schematic of the beam path for IXS scattering (vertical scattering geometry).

**2. Insertion device and optics hutch**

The X-ray source will be a standard SPring-8 in vacuum undulator (4.5 m long, 32 mm period, 8 mm minimum magnet gap) [19] 33 m upstream of the storage ring shield wall. Variations from the standard design were considered, but calculations [20] suggested they would only lead to modest (<25%) gains in flux below 25 keV at the cost of higher heat load (requiring re-design of the front end) and sensitive dependence of the available energies on the minimum gap (storage ring beta function). Table 1 shows the calculated source brilliance and flux for the standard undulator at different energies. Measurement at 14.4 keV showed the flux after the Si (111) monochromator was

Table 1

Nominal source brilliance and flux for a standard SPring-8, in vacuum undulator (100 mA current). From Ref. [21]. The bandwidth for the "Flux" column is  $1.3 \times 10^{-4}$ , for Si (111)

Energy (keV)	Brilliance ( $s/mm^2/mrad^2/0.1\%BW$ )	Flux (photons/s/ Si(III))	Flux (photons/s/ meV)
13.8	$1.8 \times 10^{19}$	$1.0 \times 10^{14}/2 \text{ eV}$	$5.0 \times 10^{10}$
17.8	$2.2 \times 10^{19}$	$1.2 \times 10^{14}/2.3 \text{ eV}$	$5.2 \times 10^{10}$
21.8	$1.9 \times 10^{19}$	$9.6 \times 10^{13}/2.8 \text{ eV}$	$3.4 \times 10^{10}$
23.7	$1.7 \times 10^{19}$	$8.6 \times 10^{13}/3.1 \text{ eV}$	$2.8 \times 10^{10}$
25.7	$1.6 \times 10^{19}$	$7.8 \times 10^{13}/3.3 \text{ eV}$	$2.4 \times 10^{10}$

approximately a factor of two reduced from the tabulated values.

The majority of the elements in the front end and optics hutches will be standard SPring-8 components [22,23]. However, we will use a cryogenically cooled Si (111) monochromator, as a prototype has been recently demonstrated at SPring-8 [24]. The optics hutch has space for lenses and/or additional filters to be installed upstream of the monochromator, while an in vacuum slit and a flux measurement device will be placed downstream of the monochromator.

**3. Inelastic X-ray scattering**

The inelastic X-ray scattering instrument is essentially a three-axis spectrometer with the main components being a monochromator, sample goniometer and an analyzer. We have chosen to use a backscattering monochromator similar to Refs. [7,8]. Other monochromator designs (e.g. [25]) were considered, and are used for IXS at APS [9,10]. However, the difficulties associated with accommodating the finite (though small) angular divergence of the X-ray beam reduce the throughput of these designs as compared to a single back reflecting crystal: relative losses of about a factor of two were expected at low ( $\sim 15$  keV) energies and a factor of 4 or more at higher energies (above 20 keV).

The use of a backscattering monochromator has two important consequences for the remainder of the spectrometer. The first is that it is necessary to use the thermal expansion of the Si crystals to vary the measured energy

Table 2

Parameters for Si back-reflections near room temperature. Note that this has been calculated based on [34,35] using code based on [36]. However, the form factors in [34] extend only to momentum transfers  $< 19 \text{ \AA}^{-1}$  so these values are extrapolated. Note tabulated widths are Darwin widths, and the FWHM is usually slightly (about 12%) larger. The angular acceptances ( $\Delta\theta$ ) are at different values of  $\delta = \pi/2 - \theta_B$

Reflection	Energy (keV)	$d$ (Å)	$\Delta E/E$	$\Delta E$ (meV)	$\Delta\theta$ (μrad) $\delta = 0.5$ mrad	$\Delta\theta$ (μrad) $\delta = 0.3$ mrad
Si (5 5 5)	9.885	0.6271	$1.5 \times 10^{-16}$	14.5	> 700	> 1000
Si (7 7 7)	13.839	0.4479	$3.4 \times 10^{-7}$	4.8	> 700	> 1000
Si (8 8 8)	15.816	0.3920	$2.6 \times 10^{-7}$	4.1	> 500	> 1000
Si (9 9 9)	17.795	0.3484	$1.0 \times 10^{-7}$	1.8	200	800
Si (11 11 11)	21.750	0.2851	$3.6 \times 10^{-8}$	0.80	72	120
Si (12 12 12)	23.725	0.2613	$3.1 \times 10^{-8}$	0.75	62	103
Si (13 13 13)	25.701	0.2412	$1.4 \times 10^{-8}$	0.35	28	47
Si (15 15 15)	29.656	0.2090	$5.0 \times 10^{-9}$	0.15	10	17

transfer (not an angular scan). The lattice constant will change by about 2.5 parts in  $10^6/K$  near room temperature, so temperature scans with  $\sim$ mK precision and few degree range become necessary. The feasibility of such scans has been demonstrated by the ESRF group [8]. Another consequence of the backscattering geometry is that the monochromatic beam is reflected nearly on top of the incident beam. In order to separate them, we will use a pair of Si 111 crystals to shift the beam after the backscattering monochromator vertically by 370 mm (see Fig. 1).

A bent cylindrical mirror will be used to focus the beam onto the sample position (a 9:1 focusing geometry). The beam spot size at the sample should be about  $150 \mu\text{m}$  in the vertical by  $100 \mu\text{m}$  in the horizontal, full width a half maximum (FWHM), where the vertical size is dominated by the slope error of the mirror ( $\leq 3 \mu\text{rad rms.}$ ). This small spot size will allow both the investigation of small samples and help minimize geometric contributions to the spectrometer energy resolution.

The analyzer (and monochromator) crystals will use the Si (nnn) family of back-reflections, as at other beamlines [7,8], since they allow the greatest flexibility. Relevant parameters are given in Table 2. The analyzer crystals will be fabricated (by an external company) using a method similar to that discussed in Ref. [26], where small blocks

of perfect silicon ( $0.6 \times 0.6 \times 3 \text{ mm}^3$ ) are glued to a spherically curved substrate. All of the tolerances for such an analyzer become easier the closer one approaches the exact backscattering. However, then one requires long path lengths to separate the scattered and analyzed X-ray beam. Our spectrometer will have a 3 m vertical arm covering scattering angles up to  $180^\circ$  (momentum transfers up to about  $15 \text{ \AA}^{-1}$ ). However, this is expected to provide not better than 3–4 meV energy resolution (e.g. using the Si (999) reflection). A longer, 10 m, arm with a horizontal scattering plane should provide  $\sim 1$  meV energy resolution (Si (11 11 11) or Si (13 13 13)). The beamline has been deliberately designed to maximize the available scan range of this arm to about  $55^\circ$  ( $> 10 \text{ \AA}^{-1}$ ). There is also potential to mount analyzer crystals on the horizontal arm at 6 m from the sample position, but this will not be commissioned until a later stage of beamline development.

The sample mounting will include a standard Eulerian cradle (specifications as for a Huber 512.1) and some independent stages. While in the initial stage of the operation, a relatively lightweight closed cycle He cryostat will be used to provide the sample environment, facilities for mounting heavier objects (e.g. a cryostat for low temperature work, or high field work, or a pressure cell) are included in the present design: some sample stages can accept a load up to  $\sim 200$  kg, and the clearance at the sample can be

Table 3

Some low-lying nuclear resonances that are interesting for synchrotron NRS experiments. Alpha is the internal conversion coefficient

Isotope	Transition energy (keV)	Lifetime (ns)	Alpha	Natural abundance (%)
$^{181}\text{Ta}$	6.21	8730	71	100
$^{169}\text{Tm}$	8.41	5.8	220	100
$^{83}\text{Kr}$	9.40	212	20	11.5
$^{57}\text{Fe}$	14.4	141	8.2	2.2
$^{151}\text{Eu}$	21.6	13.7	29	48
$^{149}\text{Sm}$	22.5	10.4	$\sim 12$	14
$^{119}\text{Sn}$	23.9	25.6	$\sim 5.2$	8.6
$^{161}\text{Dy}$	25.6	40	$\sim 2.5$	19

expanded to 350 mm in all directions (horizontal scattering geometr).<sup>1</sup>

#### 4. Nuclear resonant scattering

Nuclear resonant scattering (NRS) relies on the presence of a low-lying excited state (Mössbauer transition) in the nucleus of a particular element. A list of some of the possible nuclear transitions is given in Table 3. Several different techniques may be used to investigate sample dynamics on different energy scales. These may be divided into techniques that require that the sample contain resonant isotope and those that may be used for any sample. Specific techniques for resonant samples include inelastic nuclear absorption measurements [17,18] (giving information about phonon densities of states) and nuclear forward scattering [27]. For non-resonant samples, it is possible to do meV resolved IXS using a nuclear analyzer [28] and ~neV resolution time domain interferometry experiments [29]. Experiments on resonant samples typically have relatively large count rates, while those on non-resonant samples have been count rate limited and are particularly interesting at SPring-8.

Common to nearly all NRS techniques, is the need for the storage ring to operate in a timing mode, with large (say >20 ns) intervals between successive X-ray pulses. This permits the use of time gating (delayed coincidence techniques) to separate the nuclear scattering, which is slow (occurs on a time scale set by the nuclear lifetime) from the electronic scattering which occurs quickly (<ps). Relevant parameters for SPring-8 are the electron bunch length, about 70 ps (FWHM), the rf frequency, 508.58 MHz (so the minimum bunch spacing is about 2 ns) and the ring circumference, 1436 m (corresponding to a period of 4.8  $\mu$ s). The present maximum current/bunch is about 1 mA and the ring operates approximately half of the time in some sort of mode that may be used for nuclear scattering measurements.

Two hutches (NRS-1 and NRS-2) will be optimized for nuclear resonant scattering experiments. The first hutch will be primarily for high-resolution optics (e.g. [25,30,31]) while the second hutch will be for samples. This separation is to allow access to the sample without any disturbance to the high-resolution optics. Stages in the second hutch will allow simple diffraction experiments and positioning of the samples. A heavy-duty motorized table will also permit *xz* positioning of large (>200 kg) objects (e.g. cryostats or magnets). The detectors and electronics will be similar to those used at other NRS beamlines [32].

<sup>1</sup> However, moving the detector very far from the sample (out of the focus of the analyzer crystal) can both degrade energy resolution and reduce the count rate.

#### 5. Conclusion

We have described the design of a new facility for the investigation of sample dynamics. While being similar to some existing facilities [8–10,14–16], it will provide new capabilities due both to the design of the beamline and the high flux available from the SPring-8 storage ring.

#### Acknowledgements

AB is pleased to thank R. Ruffer and A.I. Chumakov for experience at ID18 of ESRF that greatly facilitated the design of this beamline. He is grateful to F. Sette and M. Kirsch for a tour of their IXS beamlines at ESRF. The authors are grateful to the technical and administrative staff of SPring-8 for making this project feasible.

#### References

- [1] ESRF, BP220, F-38043 Grenoble Cedex, France. <http://www.esrf.fr/>
- [2] APS, Argonne National Laboratory, Argonne, Illinois, 60439, USA. <http://www.aps.anl.gov/>
- [3] SPring-8, 323-Mihara, Mikazuki-cho, Ako-gun, Hyogo-ken, 679-5198, Japan. <http://www.spring8.or.jp/>
- [4] See the SPring-8 Beamline Handbook (in English), Available through the Users Office.
- [5] E. Burkel, Springer Tracts in Modern Physics, 125, Springer, Berlin, 1991.
- [6] E. Gerdau, H. de Waard (Eds.), submitted for publication.
- [7] E. Burkel, J. Peisl, B. Dorner, Europhys. Lett. 3 (1987) 957.
- [8] F. Sette, G. Ruocco, M. Kirsch, U. Bergmann, C. Mascivecchio, V. Mazzacurati, G. Signorelli, R. Verbini, Phys. Rev. Lett. 75 (1995) 850 see also a literature search on the above authors, especially F. Sette, for more references.
- [9] M. Schwoerer-Böhning, A.T. Macrander, D.A. Arms, Phys. Rev. Lett. 80 (1998) 5572.
- [10] M. Schwoerer-Böhning, A.T. Macrander, P.M. Abbamonte, D.A. Arms, Rev. Sci. Instrum. 69 (1998) 3109.
- [11] Beamline responsible is M. Kirsch.
- [12] E. Gerdau, R. Ruffer, H. Winkler, W. Tolksdorf, C.P. Klages, J.P. Hannon, Phys. Rev. Lett. 54 (1985) 835.
- [13] E. Gerdau, H. de Waard (Eds.), submitted for publication, and references therein.
- [14] R. Ruffer, A.I. Chumakov, Hyp. Int. 97/98 (1996) 589.
- [15] Sector 3, SRI Cat, Beamline Responsibilities E.E. Alp, W. Sturhahn. See <http://www.aps.anl.gov/sricat/3id.html>.
- [16] See the SPring-8 Beamline Handbook (in English), Available through the Users Office. Y. Yoda, Beamline contact person.
- [17] M. Seto, Y. Yoda, S. Kikuta, X.W. Zhang, M. Ando, Phys. Rev. Lett. 74 (1995) 3828.
- [18] W. Sturhahn, T.S. Toellner, E.E. Alp, X. Zhang, M. Ando, Y. Yoda, S. Kikuta, M. Seto, C.W. Kimball, B. Dabrowski, Phys. Rev. Lett. 74 (1995) 3832.
- [19] H. Kitamura, J. Synchrotron Rad. 5 (1998) 184.
- [20] H. Kitamura, unpublished.
- [21] H. Kitamura, SPring-8 Insertion Device Handbook.
- [22] Y. Sakurai, M. Oura, S. Takehashi, Y. Hayashi, H. Aoyagi,

- H. Shiwaku, T. Kudo, T. Mochizuki, Y. Oikawa, *J. Synchrotron Rad.* 5 (1998) 1195.
- [23] S. Goto, M. Yabashi, H. Ohashi, H. Kimura, K. Takeshita, T. Uruga, T. Mochizuki, Y. Kohmura, M. Kuroda, M. Yamamoto, Y. Furukawa, N. Kamiya, T. Ishikawa, *J. Synchrotron Rad.* 5 (1998) 1202–1205.
- [24] T. Mochizuki et al., unpublished.
- [25] T. Ishikawa, Y. Yoda, K. Izumi, C.K. Suzuki, X.W. Zhang, M. Ando, S. Kikuta, *Rev. Sci. Instrum.* 63 (1992) 1015.
- [26] C. Masciovecchio, U. Bergmann, M. Kirsch, G. Ruocco, F. Sette, R. Verbeni, *Nucl. Instrum. Meth. B* 111 (1996) 181 and B 117 (1996) 339.
- [27] J.B. Hastings, D.P. Siddons, U. van Bürck, R. Hollatz, U. Bergmann, *Phys. Rev. Lett.* 66 (1991) 770.
- [28] A.I. Chumakov, A.Q.R. Baron, R. Ruffer, H. Grünsteudel, H.F. Grünsteudel, A. Meyer, *Phys. Rev. Lett.* 76 (1996) 4258.
- [29] A.Q.R. Baron, H. Franz, A. Meyer, R. Ruffer, A.I. Chumakov, E. Burkel, W. Petry, *Phys. Rev. Lett.* 79 (1997) 2823–2826.
- [30] T.S. Toellner, T. Mooney, S. Shastri, E.E. Alp, in: J. Arthur (Ed.), *Optics for High-Brightness Synchrotron Beamlines*, 1992, pp. 218–222.
- [31] A.I. Chumakov, J. Metge, A.Q.R. Baron, H. Grünsteudel, H.F. Grünsteudel, R. Ruffer, T. Ishikawa, *Nucl. Instrum. Meth.* 383 (1996) 642.
- [32] See the review by A.Q.R. Baron, in E. Gerdau, H. de Waard (Eds.) *Hypofine Interactions*, in press.
- [33] D.T. Cromer, D. Liberman, *J. Chem. Phys.* 53 (1970) 1891–1898.
- [34] D.T. Cromer, D. Liberman, *J. Chem. Phys.* 59 (1970) 1891–1898.
- [35] D.T. Cromer, J.B. Mann, *Acta Cryst A* 24 (1968) 321.
- [36] W.H. McMaster, N.K.D. Grande, J.H. Mallet, J.H. Hubbell, *Lawrence Radiation Laboratory, Compilation of X-ray Cross Sections*, 1969.
- [37] S. Brennan, P.L. Cowan, *Rev. Sci. Instrum.* 63 (1992) 850.